JOURNAL OF MATERIALS SCIENCE **40** (2005) 1485–1493

Fabrication of a composite powder and its application as an active brazing alloy

M. BROCHU
Metals and Materials Engineering, McGill University, 3610 University Street, Montreal, Quebec, Canada, H3A 2B2

M. D. PUGH
Mechanical Engineering, Concordia University, 1455 blvd. De Maisonneuve West, Montreal, Quebec, Canada, H3G 1M8

R. A. L. DREW
Metals and Materials Engineering, McGill University, 3610 University Street, Montreal, Quebec, Canada, H3A 2B2

A copper-based active brazing alloy containing a high titanium content was produced by an electroless coating technique. Particles with a narrow density distribution were produced by deposition of nano-copper on a fine titanium powder. Both conventional titanium powder and sponge titanium were studied. The effects of pH and time on copper deposition were investiguated. Higher pH was found to increase the quantity of copper deposited. Using multiple depositions, a copper-titanium ratio of 75 wt% copper-25 wt% titanium could be achieved after several platings for pH varying between 12 and 12.8. The particle size distribution of the composite powder shows uniform growth of the copper shell and no agglomeration under pH 12. Major agglomeration of the final powder was observed for a bath pH of 12.8. Complete melting of the composite powder has been studied by DSC and the sessile drop technique. Melting began within the diffusion zone formed at the interface through the $Cu_4Ti \rightarrow Cu(s) + L$ peritectic reaction that occurs at 885°C. The melting process continued by successive peritectic reactions and dissolution of the remaining elements of the diffusion couple. The wetting behavior of this alloy was evaluated on different ceramic substrates (Al_2O_3, Si_3N_4) and found to be similar to literature observations.

1. Introduction

The application of ceramics in everyday life has significantly increased during the last 20 years due to an impressive technological improvement in ceramic processing. The more common ceramics are oxides, which includes alumina and zirconia for example. Oxides possess interesting characteristics like high melting temperature, chemical resistance and electrical resistance [1]. Silicon nitride has developed rapidly because it possesses very attractive properties, such as wear resistance, high temperature mechanical properties and inertness to various environments [2]. However, the brittle behavior of ceramics cannot be forgotten and another design strategy started to be applied in the 80's, which was joining ceramic pieces to metal in order to form a final component possessing better properties for applications in diverse fields [3].

It is well known that ceramic materials are generally poorly or even non-wetted by molten metal. One way to overcome this problem is by using an active liquid metal which will destabilize the covalent, or ionic bonds of the ceramic, producing at the same time, an intermediate reaction layer. This intermediate reaction layer is now wetted by molten metal [4, 5]. The most popular element added to low melting point metals to produce an active alloy is titanium [6]. Ceramic brazing requires such an active brazing alloy (ABA) to overcome the wettability problem. It is possible to find commercially available ABA, like TiCuSil® for example, produced by Wesgo Metals. However, as the demand for brazing alloys, with improved properties is always increasing, new processing techniques and new chemical compositions are being sought and studied. For the development of new compositions, one easy way of producing synthetic, laboratory scale quantities of ABA is by powder mixing (for the fabrication of paste for example). However, with the combination of various elemental powders, homogeneity could become an issue if there is a significant density difference between the different powders used [7]. Table I summarizes the density of different alloying elements commonly used in active brazing alloy composition. Using fine powders with similar densities usually minimizes this segregation during powder mixing [7].

Due to this limitation, powder coating becomes an attractive method for producing alloyed particles. The

TABLE I Density of elements usually utilized in filler metals

Element	Density (g/cm^3)	Element	Density (g/cm^3)
Copper	8.96	Tin	7.3
Silver	10.5	Indium	7.31
Gold	19.3	Titanium	4.5
Nickel	8.9	Zirconium	6.49

density and composition of the coated powder can be adjusted by controlling the thickness of the coating deposited at the surface (as a function of the density of the element deposited). In order to form an exotic chemical composition, powder mixing is the simplest, most effective technique for incorporating different powders having similar properties in terms of density and size. In other situations, one of the two main powder-coating techniques, electro- and electroless plating, may prove more suitable [8].

The electroplating technique implies the application of an electric current through a chemical bath, in which the powder to be coated is used as the anode and the metallic anions are discharged to form a film. This technique produces coatings on electrically conductive substrates only [8, 9]. The coating is often non-adherent and must be processed with care. Electroless plating (also referred to as autocatalytic plating) is very different, as no external electrical current source is needed. Also, the final deposit is less porous and re-entrant surfaces can also be coated using this technique. The metallic coating is produced by chemical reduction of a metallic salt by a reducing agent in the plating bath [9]. A major advantage over electrolytic plating is that any surface can be plated after an activation treatment (if the surface is not conductive) [9]. The most common pretreatment known is the stannous chloride/palladium reaction. This treatment leaves a conductive metallic deposit at the surface, which is then used as the precipitation site for the metallic reduction [10].

In addition to the metallic salt ($CuSO_4$ in the case of electroless Cu), the chemistry of the plating bath is composed of formaldehyde as reducing agent, EDTA as metallic salt complexant and other additives for bath stabilization [9]. The Cu reduction reaction (Equation 1) is performed in a basic bath where the pH is adjusted with NaOH.

$$Cu^{2+} + 2HCHO + 4OH^- \longrightarrow Cu^0 + H_2 + 2H_2O + 2HCO_2^- \quad (1)$$

Due to the nature of the reaction, plating is self-sustaining as long as the chemical bath is not exhausted or decomposed. The chemical compounds present in the plating solution have various effects on the plating deposit morphology, the rate of metallic deposition, and the amount of Cu available for deposition.

The objectives of this work were to investigate the possibility of coating titanium and sponge titanium powders with copper using multiple electroless coating depositions and evaluate the possibility of using this composite powder as an active brazing alloy for ceramic joining.

TABLE II Chemical composition of electroless bath

Copper (II) sulfate, pentahydrate	$CuSO_4 \cdot 5H_2O$	8 g/L
EDTA, disodium salt	$C_{10}H_{14}O_8N_2Na_2 \cdot 2H_2O$	32 g/L
2,2′-Dypyridyl	$C_{10}H_8N_2$	20 mg/L
Potassium hexacyanoferrate	$K_4Fe(CN)_6 \cdot 3H_2O$	60 mg/L
Formaldehyde, 37% solution	HCHO	7 ml/L

2. Experimental procedure

2.1. Powder coating

Both of the titanium powders used were 99% pure with a particle size of −325 mesh. For the purpose of this work, 100 g of powder were cleaned and activated prior to coating because of the surface film of oxide. The activation steps are identified as follows: (1) the powder was immersed in acetone in an ultrasonic bath for 15 min, (2) sensitization was done in a slightly acidic solution (HCl) containing tin chloride and (3) activation was performed by immersion of the powder in a solution of palladium chloride.

In order to build up a sufficient copper coating thickness, iterative depositions were carried out and a new bath solution was used each time. The composition of the electroless chemical bath is presented in Table II. The copper plating was performed in a 1 L bath for 15 g of powder. Tests were carried out at various pH between 12 and 12.8 using NaOH in order to optimize the quality of copper deposit. Initial times of 5, 10, 20, 40 and 60 min were used to study plating kinetics.

Between each plating stage, the copper coating from 5 samples was dissolved in high purity hydrochloric acid. The copper content was analyzed by atomic absorption spectroscopy (Perkin Elmer 3110) to determine the total weight deposited as a function of the number of coatings. The powder morphology as well as the precipitate quality was evaluated with SEM (Hitachi S-4700 and JEOL-840). The particle size distribution of the coated powder was studied as a function of coating build-up using the X-ray sedimentation technique (Sedigraph 5000).

The melting behavior of the powder was determined by Differential Scanning Calorimetry (Netzsch DSC 404C) using ultra high purity Ar gas as a protective atmosphere. A niobium sheeting was inserted in the Al_2O_3 crucible to avoid contact between the molten active brazing alloy and the ceramic.

The wetting behavior of this binary ABA was evaluated on alumina and silicon nitride ceramic substrates at various temperatures using the sessile drop technique in a horizontal tube furnace. The composite powder was cold pressed into a pill in a 3.2 mm diameter steel die under a pressure of 100 MPa. The wetting behavior on alumina was tested at 950 and 1025°C and for the silicon nitride at 950°C. In each case, the sample was inserted in the center of the hot zone prior to heating in order to simulate the heating stage in a brazing process. The samples were heated at 10°C/min and then soaked at the test temperature for 30 min. Photographs were taken at different intervals to evaluate the change of wetting angle with time. Prior to heating, a vacuum of 5×10^{-5} Torr was applied followed by back filling with ultra high purity argon which was used as a static atmosphere during the experiment.

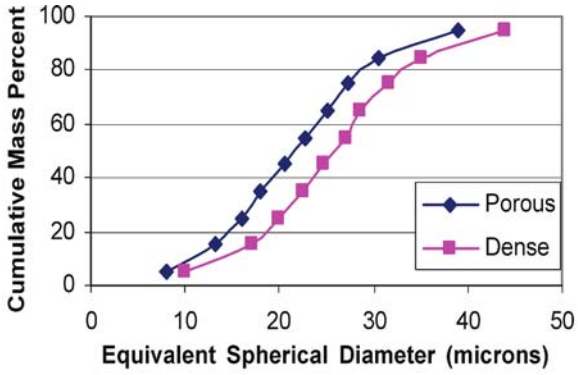

(A)

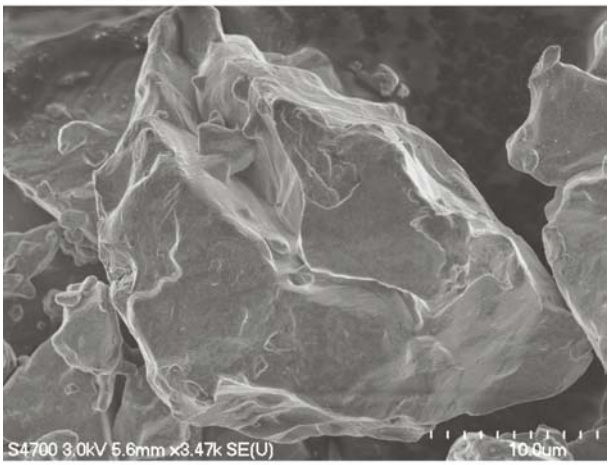

(B)

Figure 1 Particle size distribution of dense and sponge Ti powders (A) and micrograph of dense Ti particles (B).

3. Results

3.1. Starting material

Fig. 1A presents the particle size distribution of the dense and porous as-received titanium powders. Both powders have similar distributions except that the porous powder size is slightly finer. The d_{50} for the dense and porous powders are respectively 26 and 22 μm. Fig. 1B shows a picture of the dense powder prior to the plating process. Many facets are present. The numerous edges play an important role during the plating process as they are more favorable for deposition. The surface area of the powder was measured with the Brunauuer, Emmett and Teller (BET) technique to compare the possible effect of surface area on the plating rate. The surface area obtained for the dense and the porous powders was 0.37 g/m^2 and 0.42 g/m^2 respectively. For a similar difference in surface area, such as in this case, it has been shown that the plating rate is not really influenced by this parameter [11].

3.2. Powder pre-treatment

Before starting to describe the results obtained during the fabrication of this composite powder, it is important to emphasize the significance of the pretreatment. Due to the high affinity of titanium for oxygen, titanium powder possesses a non-conductive natural oxide surface film. As the electroless plating technique requires a conductive surface to allow exchange of surface electrons, the process was not successful in the case of powders without pre-treatment. To obtain a conductive surface, a stannous chloride/palladium chloride treatment was applied on the powder. XRD analysis did not show any trace of palladium residing on the powder after the pre-treatment.

3.3. Effect of pH on deposition

The electroless deposition of copper is usually performed in basic solutions when using a sulfate bath. The pH of the chemical bath was varied from 12 to 12.8. This small pH difference produces a major change in the deposit morphology. The electroless process is a technique in which atomic copper is precipitated from a salt bath solution. Fig. 2 presents high magnification micrographs of nano-cristalline copper deposits produced at pH 12 and 12.8. At the lower pH (pH = 12), the copper initially precipitates on the highest palladium concentration regions, which are usually found at the grain boundaries. Furthermore, the deposit forms rounded clusters, which grow in the three dimensions to finally produce a completely covered surface. This growth is illustrated in Fig. 2A. At higher pH (pH = 12.8), the growth of the copper precipitates does not occur in the form of spherical precipitates but more flakes-like, which grow in two dimensions, by elongation of the

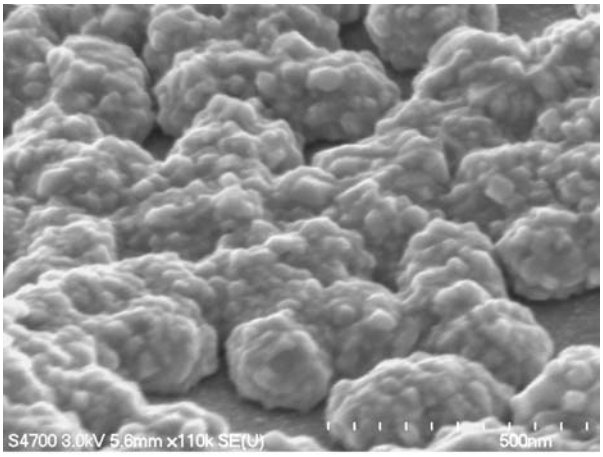

(A)

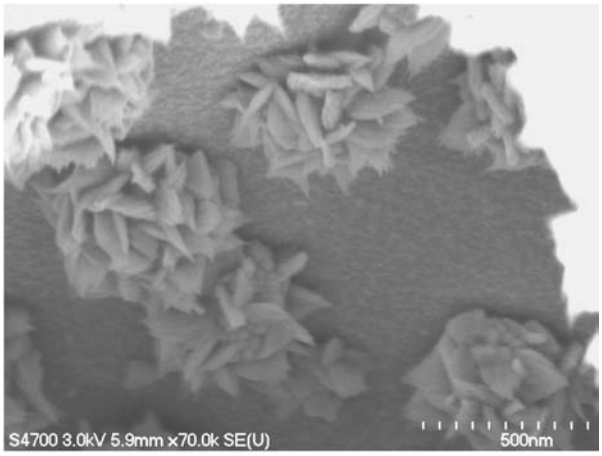

(B)

Figure 2 Micrograph of copper deposit performed at pH 12 (A) and pH 12.8 (B).

facets. Such change in deposit morphology is associated with the combined effect of the preferential growth of Cu-precipitates rather than nucleation of new deposition sites (reduction of nucleation site) and the presence of an additive in the bath, which alters the deposition reaction. Fig. 2B also shows that flake-like precipitation reduces the total area covered by the Cu deposit when compared to deposition performed at lower pH. However, the total coverage of the surface was obtained in subsequent plating steps. No voids were observed at the Cu-Ti interface demonstrating that full coverage of the Ti-core was achieved.

3.4. Effect of starting powder morphology

Interesting results concerning the initial powder morphology were also found. The possibility of plating into cavities is a characteristic of the electroless plating process. Fig. 3 shows, respectively, a low magnification micrograph (3A) of a porous titanium particle, and a micrograph taken looking into a pore (3B). Copper deposition is observed in the pores of the sponge titanium.

3.5. Plating iterations

The total copper content in the chemical bath used is 2.08 g/L for a concentration of 8 g/L of $CuSO_4 \cdot H_2O$. In the first instance, the effect of copper plating as a function of time was evaluated to determine the optimum plating time. Table III shows the wt% copper deposited after 5, 10, 20, 40 and 60 min. In the case of deposition performed at pH 12, the bath was never exhausted as the final color was slightly blue. However, at pH 12.8, the bath was mostly exhausted after 40 min, as the solution turned clear. From these results, a plating time of 60 min for the deposition at pH 12 and 40 min for pH 12.8 were chosen. Both plating times were kept constant for each iteration of the process.

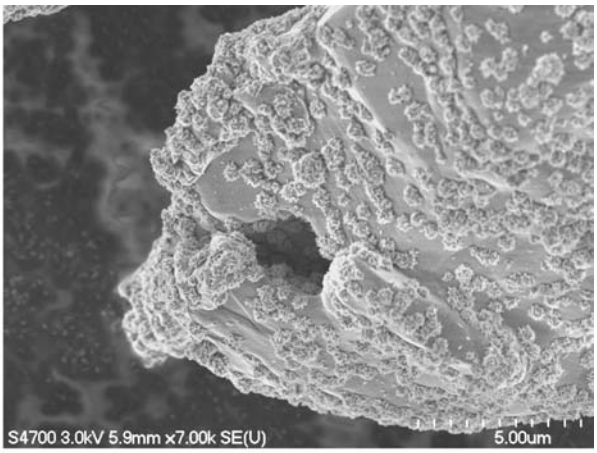

(A)

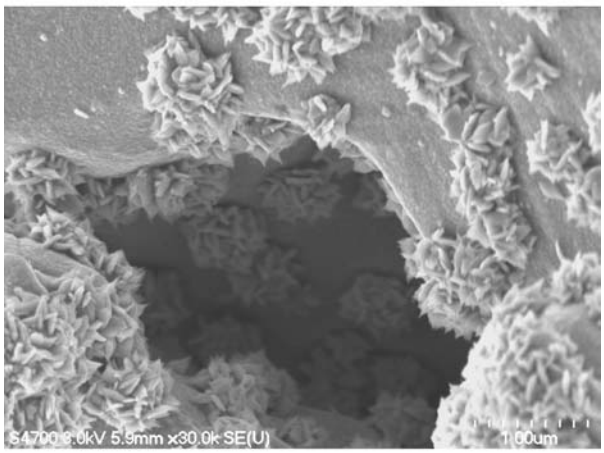

(B)

Figure 3 Copper deposition inside pore of sponge titanium particle.

TABLE III Amount of copper plated as a function of time

	pH = 12 (wt%)		pH = 12.8 (wt%)	
Deposition time (min)	Average	Std Dev	Average	Std Dev
5	5.66	0.25	9.64	1.19
10	6.16	0.17	10.36	1.51
20	6.83	0.25	10.91	0.97
40	–	–	11.36	0.85
60	8.90	0.59	11.48	0.53

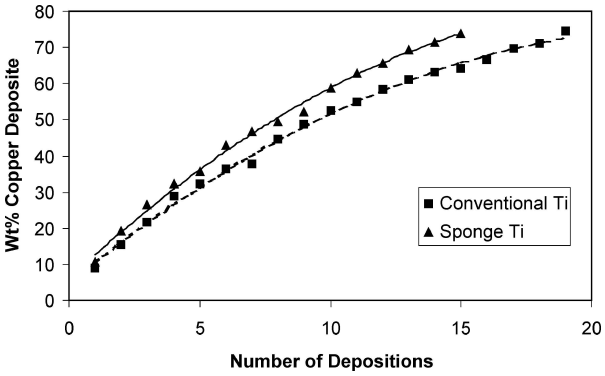

Figure 4 Amount of copper deposited as a function of plating iterations.

Fig. 4 presents the curves of the net concentration of copper on both types of powder as a function of the number of deposition steps. To obtain the target composition of 75 wt%Cu, 19 iterations were necessary when a bath solution of pH 12 was used. The higher bath pH required 15 iterations, which is one advantage of increasing the pH. In both cases, the curves follow a parabolic trend since the wt% is calculated as the ratio of the weight of copper deposited to the total weight of the powder. In both cases, the curves will ultimately reach a plateau with increasing iterations, as the mass of Ti is not negligible. This result shows the difficulty and limitation of producing filler alloy containing a low quantity of active element (starting powder) using this process alone (i.e. not using a Ti and Cu powder mixture for example).

3.6. Particle size distribution

The particle size was evaluated in order to observe if the copper coating build-up is uniform and to observe the possibility of agglomeration. The particle size distribution of the initial powder and the final composite powder coated at pH 12 is presented in Fig. 5. The starting titanium powder is representative of a Gaussian-type of distribution. The mode of the distribution is between 20–30 microns. The particle size distribution of the final

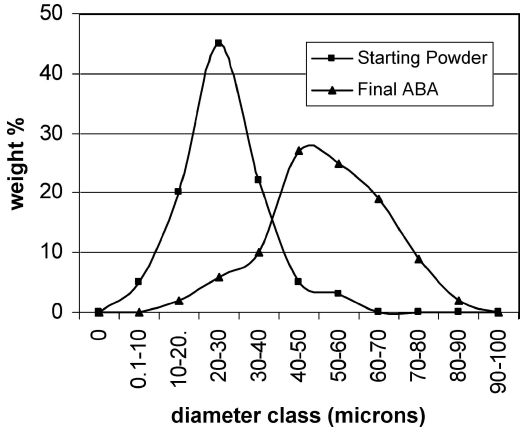

Figure 5 Gaussian distribution of composite powder plated at pH12.

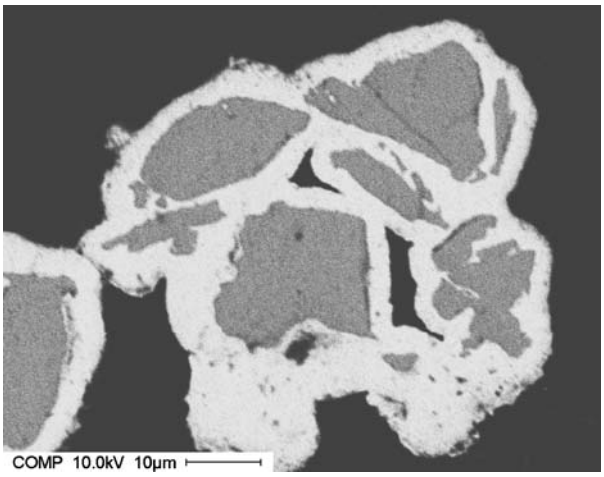

Figure 6 Back-scattered micrograph of agglomerate of particles coated at pH12.

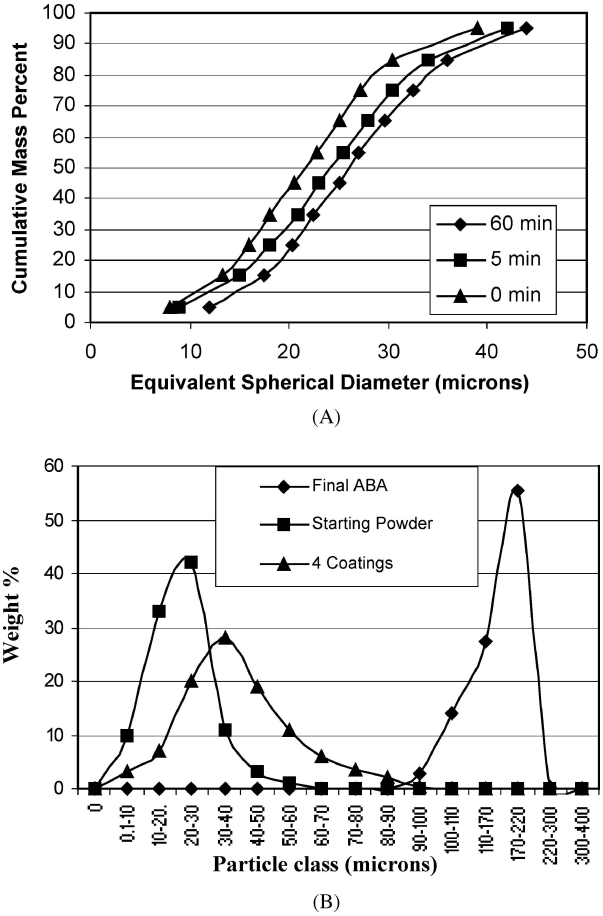

Figure 7 Effect of time (A) and iteration step (B) on particle size distribution.

ABA is shifted to the right, indicating that the particle size has increased. As opposed to the starting powder, the distribution no longer follows a Gaussian-type of distribution. The mode of the distribution cannot be as easily determined, as the difference in quantity of powder having a final size between 40 and 65 microns is not very significant. The right hand side of the particle size distribution curve of the final ABA powder, which does not decline as sharply as for a typical distribution, indicates the presence of a higher percentage of larger particles, compared to a Gaussian distribution. The larger particles are created by powder agglomeration. Fig. 6 presents a back-scattered electron image of a cross-section of such an agglomerate. The outside, lighter layer, is the copper coating and the darker core is the original titanium particle. The diameter of the agglomerate at its maximum is approx. 90 microns, which corresponds to the larger values indicated in the particle size distribution.

Fig. 7 presents the variation in particle size distribution of the porous powder plated at pH 12.8 as a function of time during the initial plating (A) and as a function of iteration step (B). After 5 min of plating, the composite powder contains 9.6 wt%Cu whilst after 60 min it contains 11.5 wt%. In Fig. 7A, the distribution curve moves to the right due to the growth of the powder diameter with quantity of copper deposited but the shape remains similar. This illustrates that no agglomeration occurs. Fig. 7B presents the initial distribution of the powder as well as its evolution after 4 and 15 platings. After 4 platings, considerable agglomeration of the particles can be observed, as the slope on the right side of the curve is not as sharp compared to the initial powder. The final particle size has been affected by severe agglomeration, where the mode of the distribution is 210 microns, as opposed to ≈45 microns for the powder plated at pH 12.

Low voltage FE-SEM coupled with EDS was used to characterize the surface of copper deposit. FE-SEM possesses the advantage over the conventional scanning electron microscope of the possibility of having sufficient beam current for EDS analysis at low voltage, which reduces substantially the interaction volume. Fig. 8 presents the EDS analysis of both powder surfaces. The surface concentration of oxygen is higher for deposits formed at higher pH, which is related to a secondary-reaction involving deposition of copper oxide instead of pure copper during plating.

3.7. Composite powder melting

In order to obtain a suitable brazing liquid from the composite powder, diffusion has to occur between the coating and the core of the powder. The binary copper-titanium phase diagram shows the presence of many intermetallics as well as a Cu-rich eutectic for a composition of 78 wt%Cu at 875°C [12]. The heat flow

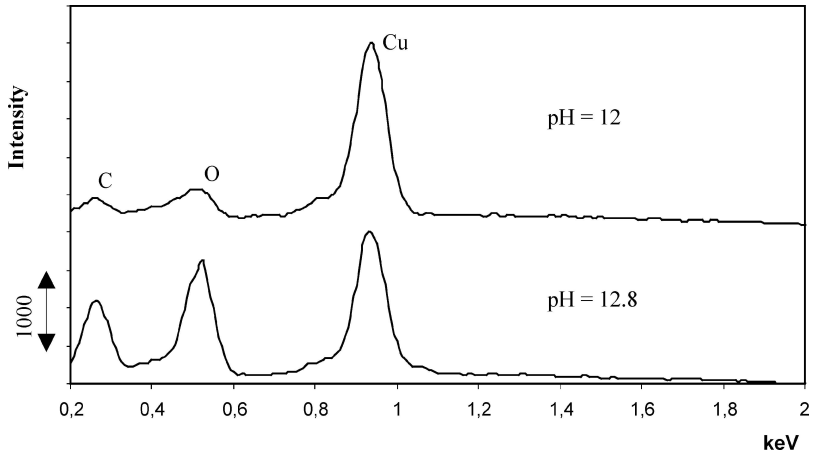

Figure 8 EDS analysis of both composite powder surfaces.

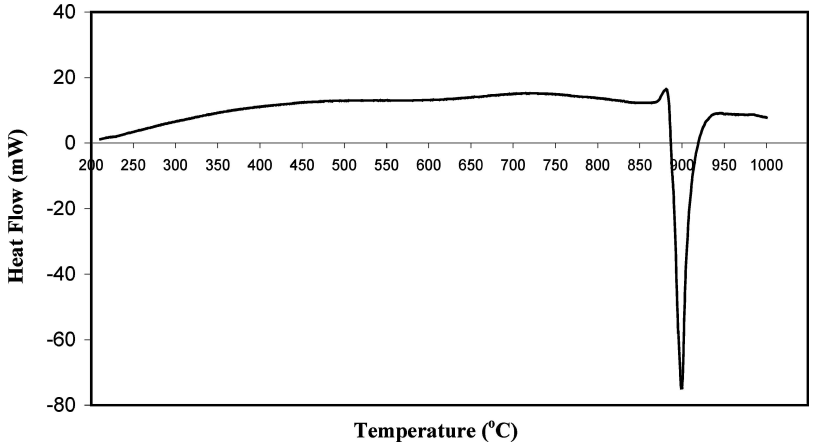

Figure 9 DSC curve of composite powder during heating stage.

during the heating stage of a sample of powder was measured with DSC and the results are presented in Fig. 9. In such analysis, melting is observed through the endothermic peak. Initial melting of the powder occurs at 880°C, which corresponds to the melting of a layer possessing the Cu-rich eutectic composition. Complete melting was obtained at 915°C. The exothermic bump observed before melting is believed to correspond to the formation of Cu_2Ti intermetallic, which is stable between 870 and 890°C.

3.8. Evaluation of wetting behavior on ceramic substrates

Ceramic brazing is achieved by furnace brazing in which the pre-applied filler metal follows the same heating cycle as the parts to be joined. As observed on the DSC experiments, diffusion occurs during the heating stage. A pill of coated powder was inserted in a wetting furnace at room temperature and was heated at 10°C/min. Pictures were taken at different time intervals to correlate the behavior of a macro sample of powder to the results obtained with the DSC. Fig. 10A is a picture of the pill at 910°C. The initial geometric form of the pill is still constant, which mean that complete melting has not yet occurred. However, Fig. 10B shows a picture of the same pill two min later, at 932°C. A complete drop has formed on the surface of the ceramic substrate. Sufficient diffusion between the copper-titanium diffusion couple and the furnace temperature gradient has been overcome which, produce total melting of the pill by 932°C. It can also be observed that the alloy instantaneously wets the ceramic substrate, i.e. contact angle lower than 90°. Due to the nature of the wetting system, spreading of the molten drop will be expected to occur resulting from the reaction between molten ABA and the Si_3N_4 substrate.

The wetting behavior of the composite powder was tested on different ceramic substrates in order to compare the contact angle values obtained with values published in the literature. Alumina and silicon nitride ceramics were selected as these are commonly brazed. The temperatures used were only slightly higher than the melting point of the composite powder, in order to see the rate of decrease of contact angle as it is well known that a molten metal, with high active element content, typically possesses a very low contact angle and the equilibrium contact angle is reached rapidly [13]. The wetting curves are presented in Fig. 11. The final contact angle for alumina is around 60°, independently on the tested temperature. The spreading of the drop is clearly shown for a sample tested at 950°C. As the contact angle does not change for the test performed at 1025°C, spreading occurred during the heating period between melting and the test temperature. Contact angle equilibrium was achieved before the test

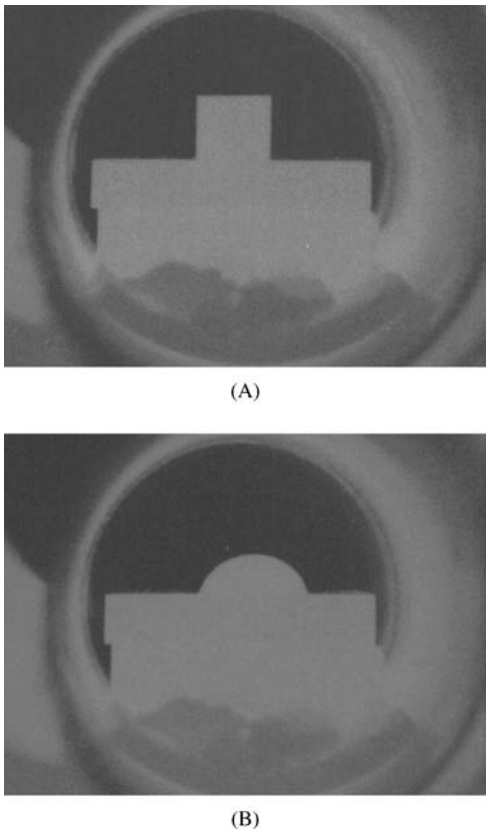

Figure 10 In situ photograph of composite powder pill on Si_3N_4 substrate at 930°C (A) and 950°C (B), respectively.

temperature is reached and is observed as similar values were measured for $t = 0$ and for $t = 30$ min. From the literature, the contact angle between copper-titanium alloy and Al_2O_3 decreases rapidly above the tested temperatures [14]. The results obtained are thus similar to previous researchers values. For silicon nitride, the equilibrium contact angle obtained is lower than that for alumina. The equilibrium contact angle for this system is around 18° for samples tested at 950°C. For higher temperatures, the contact angle decreases rapidly and becomes nearly zero, at which point it becomes very hard to measure. This behavior was expected, as the titanium concentration is very high. Filler metal with lower active element concentration has also been found to have a very low equilibrium contact angle. It also decreases rapidly with the concentration of active element. The results obtained for the Si_3N_4/75Cu-25Ti system are also similar to literature [15].

4. Discussion

The active brazing alloy produced in this work possesses a higher concentration of active element than conventional ABA. Even if this composite powder can be directly used to braze ceramics, this alloy was developed as precursor for more complex chemistries by powder mixing. Homogeneity of a powder mix is a function of the density of its components. Ti possessing a much lower density than many transition metals, commonly used as a base-alloy (see Table I for comparison of densities). Such composite powder will help to prevent segregation during mixing. In order to produce a composite powder, the electroless plating process has certain advantages compared to powder mixing and the electrolytic process. The metal is deposited uniformly on all surfaces exposed to the solution, not only at the outer surface. Hence an advantage is that the amount of copper plated may be increased when the powder contains open porosity. The mass of a titanium sponge particle is lower than that of a conventional titanium particle of similar particle size due to the presence of pores. Thus the final density of the plated powder will be higher for the sponge powder for a similar particle size. This can produce a powder with a similar target composition but smaller in size compared to using conventional titanium powder as the core.

The morphology of the copper deposit has been shown to be greatly influenced by the chemical composition of the plating bath; from rounded nucleation sites (three-dimensional growth) to faceted (two-dimensional growth). Previous researchers have reported that the composition of the chemical bath may change the growth mode. Weber *et al.* [16] mentioned that a cyanide-containing bath produces a strong decrease in the nucleation rate, which changes the growth mode from 3D (for the additive-free bath) to 2D growth mode. Clearly developed crystals with sharp edges and flat crystal faces were observed during plating at pH

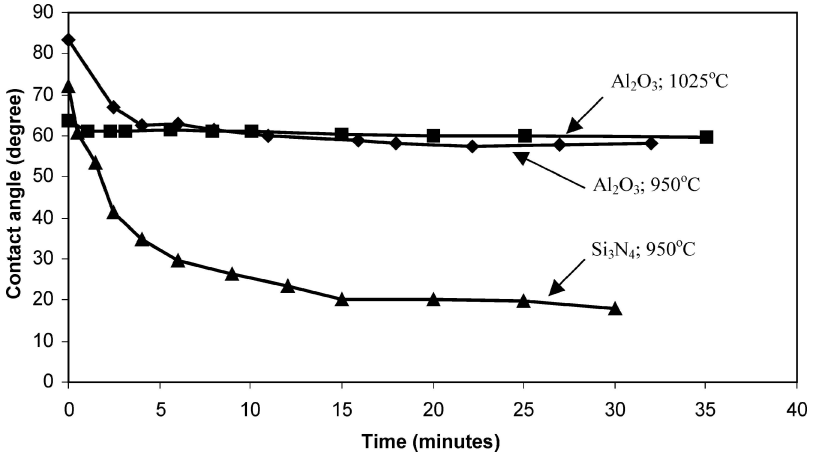

Figure 11 Contact angle of molten composite powder on Al_2O_3 and Si_3N_4 ceramic.

13. They also observed that additive-free baths produce rounded copper precipitates under pH 13. The presence of precipitates possessing flat crystal faces has to be associated with the additive which is used to avoid self-decomposition, enhance the deposition rate and improve the deposit properties. In the present work, the deposit morphology obtained for plating performed at pH of 12.8 is similar to that produced by Weber, since faceted crystals were formed. However, by lowering the pH of the bath, the copper deposit grows in three dimensions, in a similar fashion to that reportedly obtained under additive-free or accelerator-containing baths. Copper deposition under this lower pH shows a lower deposition rate, as formaldehyde oxidation occurs only at pH values above 12 and this oxidation rate is a function of pH. When the pH reaches lower values, the plating process stops altogether.

Lowering the bath pH mainly diminished the plating process efficiency. The amount of copper plated during each deposition is around 70% of the total available copper, when plating at low pH for a plating time of 60 min. The efficiency increases up to almost 100% in the case of pH 12.8 for duration of only 40 min. Because the autocatalytic process decreases the pH of the bath during plating, and the formaldehyde oxidation occurs only at or above pH 12, and the deposition occurs because of the presence of formaldehyde, the overall reaction is strongly governed by the pH of the initial bath. At lower pH, the plating reaction is stopped earlier as the reducing agent becomes inactive.

The agglomeration of the composite powder at higher pH becomes a real problem because the larger agglomerate size will create a thicker layer of filler in between the pieces to be joined. Normally, agglomeration is associated with a zeta potential of zero. This observation is valid for non-conductive materials, which exhibits a double layer formation in polar solutions. In the present case, the surface is composed of metal (electrical conductors) and no agglomeration should occur, like observed at lower pH. Agglomeration was observed during plating at higher pH, suggesting that the agglomeration problem is strongly correlated to the bath composition. Shukla *et al*. [10] have shown that CuO can be formed at the surface of the metallic copper deposit during the electroless deposition. The copper color was not observed on the powder when plated at pH of 12.8 but a color more characteristic of copper oxide was obtained. Low voltage EDS analysis has demonstrated a large variation in surface oxygen, suggesting higher oxidation of the deposit for higher processing pH. In addition to the non-metallic surface, complexes can be created which promotes the formation of Van der Waals bonding, which can be strong enough to attract and link particle together by precipitation at the interface. This interface precipitation is observed by the presence of voids formed at the triple junction between particles.

The wetting behavior, as well as the interfacial reaction products, are similar to results obtained by previous researchers. Meier *et al*. have shown that the alloying method, for the case of a copper-titanium binary active alloy, does not influence the final contact angle but changes the spreading kinetic to obtain equilibrium [14]. In the present work, the complete melting point of the brazing metal has been raised from around 890°C in the case of pre-alloyed powder to around 950°C in the case of our composite powder. The alloy formation involves the formation of several intermetallic layers, which possess different melting characteristics. In the case of coated powder, melting of intermediate layers occurs before the complete melting of individual particulates.

Ceramic brazing with an active brazing alloy possessing a high active element content has shown that the thickness of the reaction layer increases much more rapidly than for brazing alloys with lower active element content [13]. Brazing operations are conventionally performed at temperatures only slightly higher than the melting point of the filler metal, to avoid superheating of the filler metal. Raising the "melting" temperature, compared to pre-alloyed powder, reduces the extent of the reaction between the ceramic and the filler metal during the heating stage, which in turn reduces the growth of the reaction layer and better interfacial control can be achieved. The fabrication of a mixture of the composite powder and pure metal powder can also increase the melting temperature of the filler metal and change the composition. Furthermore, isothermal solidification may occur, depending on the system resulting in an improvement of the control of the reaction rate between the liquid and the ceramic substrate.

5. Conclusions

This research has demonstrated the potential for fabricating an active brazing alloy powder by building a shell of copper on a titanium particles using an electroless plating technique. This method was used primarily because deposition may be performed on non-conductive surfaces, such as titanium oxide passive film on titanium powder. Higher bath pH shows faster deposition rates, moreover, the growth morphology of the copper deposit is in the form of lamellar facets and strong agglomeration of the powder was observed after several plating iterations. At lower pH, the deposition rate is slower, the deposit grows in clusters and no agglomeration of the powder was observed. The pH of the plating influences the deposit surface composition, where the surface oxygen concentration increases with the pH. *In-situ* diffusion during the heating cycle initiates melting at 886°C and completes melting by 915°C. The behavior observed in the furnace shows that, at higher temperature than the initial melting temperature observed in the DSC, the composite powder remains in its original shape. The higher melting temperature observed in the furnace, compared to complete melting in the DSC, is associated with a larger temperature gradient. The contact angle of the filler metal on alumina and silicon nitride ceramics is similar to values obtained by previous researchers for conventional brazing alloy formulations of similar composition.

Acknowledgements

The authors would like to thank NSERC for overall funding of the project and Fonds de Recherche sur la

Nature et les Technologies and McGill University for various scholarships. The authors would also like to thanks Dr. S.F. Corbin and Mr. D. Turriff for the use of the DSC.

References

1. W. E. LEE and W. M. RAINFORTH, "Ceramics Microstructure Properties Control by Processing" (Chapman & Hall, 1994).
2. K. SUGANUMA, "Joining Non-Oxides Ceramics, Engineered Materials Handbook; Ceramics and Glasses" (ASM International, 1990).
3. J. A. FERNIE and W. B. HANSON, *Industr. Ceram.* **19**(3) (1999) 172.
4. W. TILLMANN, E. LUGSCHEIDER, R. XU and J. E. INDACOCHEA, *J. Mater. Sci.* **31** (1996) 445.
5. W. B. HANSON, K. I. IRONSIDE and J. A. FERNIE, *Acta Mater.* **48** (2000) 4673.
6. M. G. NICHOLAS, "Active Metal Brazing" (Joining of Ceramics Institute of Ceramics, Chapman and Hall, 1990).
7. F. THÜMMLER and R. OBERACKER, "An Introduction to Powder Metallurgy" (The Institute of Materials, 1993).
8. G. S. UPADHYAYA, "Powder Metallurgy Technology" (Cambridge International Science Publishing, 1997).
9. C. A. DECKERT, "ASM Handbook, Surface Engineering" (1994) Vol. 5, p. 311.
10. S. SHUKLA, S. SEAL, J. AKESSON, R. ODER, R. CARTER and Z. RAHMAN, *Appl. Surf. Sci.* **181** (2001) 35.
11. C. A. LEON, "Infiltration Processing of Metal Matrix Composites Using Coated Ceramic Particulate," Ph.D. Thesis, McGill University, 2001.
12. "ASM Handbook Alloy Phase Diagrams" (1992) Vol. 3.
13. M. G. NICHOLAS, "Joining Processes; Introduction to Brazing and Diffusion Bonding" (Kluwer Academic Publishers, 1998).
14. A. MEIER, P. R. CHIDAMBARAM and G. R. EDWARDS, *J. Mater. Sci.* **30** (1995) 3791.
15. M. NAKA and I. OKAMOTO, *Trans. JWRI* **14**(1) (1985) 29.
16. C. J. WEBER, H. W. PICKERING and K. G. WEIL, *Microstruct. Sci.* **25** (1997) 373.

Received 21 March 2003
and accepted 24 September 2004